Lawrence Berkeley Laboratory
UNIVERSITY OF CALIFORNIA

Physics, Computer Science & Mathematics Division

Presented at the XX International Conference on High Energy Physics, University of Wisconsin-Madison, Madison, WI, July 17-23, 1980

OPEN AND HIDDEN CHARM MUOPRODUCTION

A.R. Clark, K.J. Johnson, L.T. Kerth, S.C. Loken, T.W. Markiewicz, P.D. Meyers, W.H. Smith, M. Strovink, W.A. Wenzel, R.P. Johnson, C. Moore, M. Mugge, R.E. Shafer, G.D. Gollin, F.C. Shoemaker, and P. Surko

September 1980

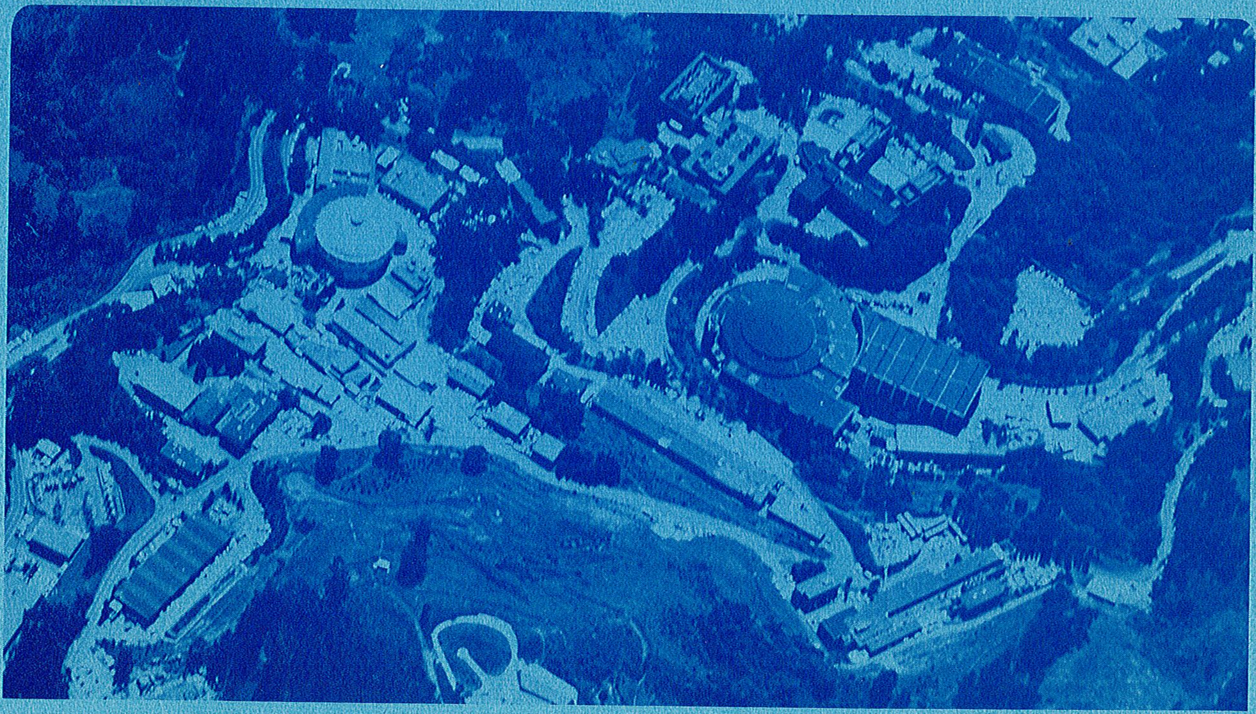

Prepared for the U.S. Department of Energy under Contract W-7405-ENG-48

LBL-11561
FERMILAB-Conf-80/84-exp
COO-3072-116

OPEN AND HIDDEN CHARM MUOPRODUCTION

A.R. Clark, K.J. Johnson, L.T. Kerth, S.C. Loken, T.W. Markiewicz, P.D. Meyers, W.H. Smith, M. Strovink, and W.A. Wenzel

Physics Department and Lawrence Berkeley Laboratory
University of California, Berkeley, California 94720

and

R.P. Johnson, C. Moore, M. Mugge, and R.E. Shafer

Fermi National Accelerator Laboratory,
Batavia, Illinois 60510

and

G.D. Gollin[a], F.C. Shoemaker, and P. Surko[b]

Joseph Henry Laboratories, Princeton University
Princeton, New Jersey 08544

Presented at the XX International Conference on High Energy Physics, University of Wisconsin-Madison, Madison, Wisconsin July 17-23, 1980 by A.R. Clark

September, 1980

OPEN AND HIDDEN CHARM MUOPRODUCTION

A.R. Clark, K.J. Johnson, L.T. Kerth, S.C. Loken, T.W. Markiewicz, P.D. Meyers, W.H. Smith, M. Strovink, and W.A. Wenzel
Physics Department and Lawrence Berkeley Laboratory,
University of California, Berkeley, California 94720

R.P. Johnson, C. Moore, M. Mugge, and R.E. Shafer
Fermi National Accelerator Laboratory,
Batavia, Illinois 60510

G.D. Gollin[a], F.C. Shoemaker, and P. Surko[b]
Joseph Henry Laboratories, Princeton University
Princeton, New Jersey 08544

ABSTRACT

New results are presented on open and hidden charm and bottom production by 209-GeV muons interacting in a magnetized steel calorimeter. The upper limit on the production of Υ states by muons is $\sigma(\mu N \rightarrow \mu \Upsilon X)B(\Upsilon \rightarrow \mu\mu) < 22\times10^{-39}$ cm^2 (90% confidence level). The distributions of elastically produced ψ's are consistent with s-channel helicity conservation (SCHC) and disagree with ψ dominance. From analysis of dimuon final states the cross section for diffractive charm muoproduction is $6.9^{+1.9}_{-1.4}$ nb. The structure function $F_2(c\bar{c})$ for diffractive charmed-quark pair production is presented.

INTRODUCTION

New results are presented from 209-GeV muon interactions in the Berkeley-Fermilab-Princeton Multimuon Spectrometer at Fermilab[1]. Because of space limits on this text, we have omitted many figures and made the discussions brief. The reader should consult the references for complete details of each analysis.

LIMIT ON Υ CROSS SECTION

Our data have yielded 102 678 trimuon final state events. In every event, all three outgoing muons are fully momentum analyzed and are subject to an energy-conserving 1-C fit using the calorimetric measurement of the shower energy.

A detailed analysis of the dimuon mass spectrum results in a limit on the Υ muoproduction cross section of $\sigma(\mu N \rightarrow \mu \Upsilon X)B(\Upsilon \rightarrow \mu\mu) < 22\times10^{-39}$ cm^2 (90% confidence level). The reader is referred to the recently published report of this analysis for a detailed discussion[2].

---

[a]Now at Enrico Fermi Institute, Chicago, Illinois 60637.

[b]Now at Bell Laboratories, Murray Hill, NJ 07974.

ψ DISTRIBUTIONS

Our first results on ψ final states have been published[1]. Here we present the angular distributions of the full elastic data set and their effect on the measurement of the Q^2 distribution[3].

If we assume s-channel helicity conservation (SCHC), natural parity exchange (NPE), and no single spin flip contributions, then the angular distribution of $\psi\to\mu^+\mu^-$ is[4]:

$$W(\theta,\phi,\eta,R)=\frac{1}{1+\epsilon R}\cdot\frac{3}{16\pi}\{(1+\cos^2\theta)+2\epsilon R\sin^2\theta-\eta\epsilon\sin^2\theta\cos 2\phi\}, \quad (1)$$

where $R=\sigma_L/\sigma_T$ is the ratio of psi production cross sections by, and $\epsilon=\Gamma_L/\Gamma_T$ is the flux ratio of, longitudinally and transversely polarized virtual photons. We have inserted a factor η to monitor the size of the polarization angle asymmetry term; $\eta=1$ if SCHC and NPE are exactly obeyed.

The vector meson dominance (VMD) model of lepton scattering suggests that $R=\xi^2Q^2/m_\psi^2$. Any Q^2-dependence in the angular distribution, together with a non-uniform spectrometer acceptance in $\cos\theta$, can bias the interpretation of the overall Q^2 distribution. To study these effects the data were binned in a 4x5x3 Q^2, $|\cos\theta|$, and ϕ space. An individual mass-continuum subtraction was performed for each of the 60 bins; the resulting data were fit with the product of the angular function $W(\eta,R)$ and a propagator $P(\Lambda)=(1+Q^2/\Lambda^2)^{-2}$, under various assumptions for η, R and Λ. An additional complication is the possibility of a Q^2 dependence in the amount of nuclear matter seen by the incident virtual photon. We have fit recently summarized data[5] measuring this effect for $A\sim200$, scaled for use in Fe:

$$(A_{eff}/A)_{Fe}\equiv S(x')=(1-0.328e^{-28.3x'})^{0.760} \quad ; \quad x'\equiv\frac{Q^2}{2m_p\nu+m_p^2} \qquad (2)$$

All fits were made with $S(x')$ both included and ignored.

The results of the fits are presented in Table I; the angular data and the results of fits 1-4 are shown in Figure 1. For plotting purposes only, the data and fits have been summed over ϕ or $|\cos\theta|$. While there is little difference between fits of the general SCHC form, it is clear that the polarization angle data rule out a flat angular distribution (fit 3).

The Q^2 distribution for $\sigma_{eff}(\gamma_V N\to\psi X)$ is present in Fig. 2. Our insensitivity to the exact form of R and to the possible nuclear effects results in a propagator mass Λ between 1.9 and 2.6 GeV/c^2. The VMD prediction ($\Lambda=m_\psi$, fit 5) is ruled out. A photon-gluon-fusion (γGF) prediction has also been fit to the data (fit 7); the data fall faster than the γGF prediction. A complete discussion appears in Ref. 3.

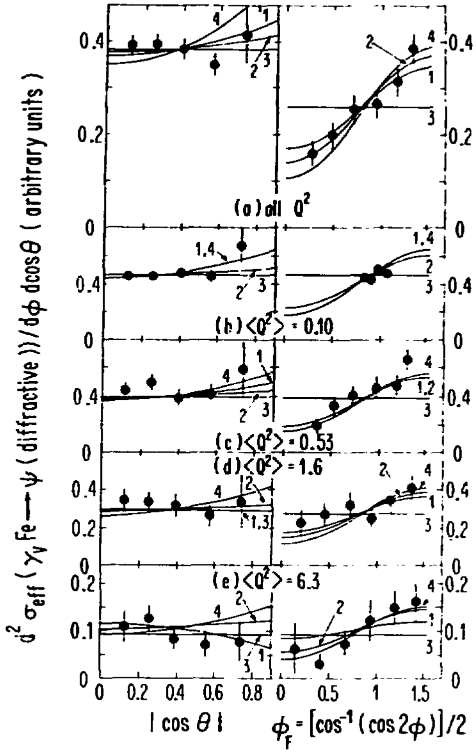

FIG. 1. Angular dependence of the effective cross section for the reaction $\gamma_V Fe \rightarrow \psi X$ (energy(X)<4.5 GeV). Data and statistical errors are presented vs. $|\cos\theta|$ (left column) and ϕ (right column), with ϕ folded into one quadrant. All data ($\langle Q^2\rangle$=0.71) are shown in (a); (b)-(e) divide the data into four Q^2 regions. Numbered solid lines exhibit the results of fits 1-4 in Table I. Fits 1, 2, and 4 are to the SCHC formula with $\sigma_L/\sigma_T=\xi^2Q^2/m_\psi{}^2$, constant, and zero, respectively; fit 3 corresponds to the production of unpolarized ψ's. Each fit is made to all the data with one adjustable normalization constant.

FIG. 2. Q^2-dependence of the effective cross section for the reaction $\gamma_V Fe \to \psi X$ ($E_X < 4.5$ GeV). Data and fits have been summed over $|\cos\theta|$ and ϕ. Statistical errors are shown. The data are fit to $(1+Q^2/\Lambda^2)^{-2}$ multiplied by the function $W(n,R)$ shown in Eqn. 1. The weak Q^2-dependence of W results from the Q^2-dependence of R and the particular average values of the angular factors $\cos\theta$ and $\cos 2\phi$. The best fits with free Λ (Table I, fit 1) and fixed Λ=3.1 (fit 5) are shown. The data are normalized so that fit 1 is unity at Q^2=0. Also exhibited is the γGF prediction (fit 7). At high Q^2, the two latter fits are displayed as a solid band, with the upper (lower) edge including (omitting) the screening factor $S(x')$.

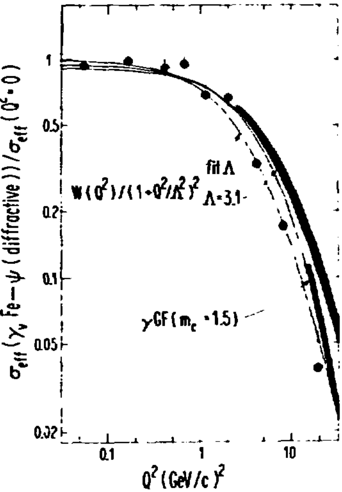

Table I. Fits to the Q^2, ϕ, and θ-dependence of the effective cross section σ_{eff} for the reaction $\gamma_V Fe \to \psi X$ ($E_X < 4.5$ GeV). Errors on the fit parameters are statistical. Fit 6 is the same as fit 1 except that W is multiplied by $(1+\epsilon R)$: Λ then parameterizes the Q^2-dependence of σ_T rather than σ_{eff}. Fit 7 compares the data integrated over ϕ and $\cos\theta$ with the Q^2-dependence predicted by γGF.

Fit No.	Function	$S(x')$	χ^2/DF	Λ(GeV/c^2)	n	ξ^2 or R
1	$W(n,R)\times P(\Lambda)$, $R=(\xi Q/m_\psi)^2$	in	45.4/56	$2.03^{+0.18}_{-0.12}$	$1.02^{+0.28}_{-0.23}$	$3.3^{+4.9}_{-3.0}$
		out	45.5/56	$2.18^{+0.18}_{-0.13}$	$1.04^{+0.28}_{-0.23}$	$4.0^{+4.8}_{-3.4}$
2	$W(n,R)\times P(\Lambda)$, R=constant	in	42.0/56	2.24±0.13	$1.09^{+0.31}_{-0.24}$	$.35^{+.26}_{-.18}$
		out	42.4/56	2.43±0.15	$1.10^{+0.31}_{-0.24}$	$.37^{+.27}_{-.22}$
3	$1\times P(\Lambda)$	in	73.3/58	2.06±0.11		
		out	73.3/58	2.22±0.13		
4	$W(1,0)\times P(\Lambda)$	in	48.6/58	2.21±0.12	≡1	≡0
		out	49.3/58	2.40±0.14		
5	$W(n,0)\times P(m_\psi)$	in	89.1/58	≡3.1	0.96±0.13	≡0
		out	68.5/58		0.93±0.14	
6	$(1+\epsilon R)\times$Fit 1	in	47.0/56	2.08±0.24	0.86±0.17	$.24^{+.61}_{-.39}$
		out	47.6/56	2.20±0.29	0.87±0.17	$.34^{+.75}_{-.43}$
7	γGF -- Q^2 projection	in	32.1/8	m_c≡1.5 GeV/c^2		
		out	14.6/8			

DIFFRACTIVE CHARM MUOPRODUCTION CROSS SECTION

The data have yielded 20072 dimuon final state events, with (81±10)% attributed to production of charmed states decaying to muons. The background from π, $K\to\mu$ decay was simulated in a model-independent fashion by using hadron muoproduction and decay parameters measured in other experiments. The background-subtracted data was fit satisfactorily with a γGF model producing D mesons, which decay semileptonically. The cross section for diffractive charm production is measured to be $\sigma_{diff}(\mu N\to\mu c\bar{c}X)=6.9^{+1.9}_{-1.4}$ nb, where the errors are systematic. A report of this analysis has been published[6].

CHARM STRUCTURE FUNCTIONS

Fig. 3 displays the ν-dependence of $\sigma_{eff}(\gamma_V N\to c\bar{c}X)$ from the analysis described in the previous section. The insensitivity of σ_{eff} to Q^2 in this range decouples its Q^2 and ν-dependence. The γGF model with gluon distribution $3(1-x)^5/x$ successfully describes the data; however, systematic uncertainties prevent the analysis from ruling out other possible models (see Ref. 7).

We define the charm structure function $F_2(c\bar{c})$ through the relation

$$Q^4\nu d^2\sigma(c\bar{c})/dQ^2d\nu=4\pi\alpha^2(1-y+y^2/2)F_2(c\bar{c}) \quad ; \quad y=\nu/\nu_{max}. \qquad (3)$$

The Q^2 dependence of $F_2(c\bar{c})$ is shown in Fig. 4 for two values of ν. At its peak $F_2(c\bar{c})$ is ~4% of F_2. The predictions of the γGF model resemble the data, but none of the models adequately fit the data.

In the energy range of the data in Fig. 5, $F_2(c\bar{c})$ is clearly scale-noninvariant for $Q^2<10$ (GeV/c)^2, or $x_B\lesssim0.07$. To model the charm contribution to F_2 for smaller photon energies, we normalize the γGF model to the data and damp it at high Q^2 by the factor $(1+Q^2/(10\ \mathrm{GeV/c})^2)^{-2}$. The resulting family of dashed curves in Fig. 5 adequately matches the data.

Table II compares the fit[9] inclusive $\partial F_2/\partial\ell nQ^2$ at fixed x_B to $\partial F_2(c\bar{c})/\partial\ell nQ^2$ augmented for charmonium production, calculated with the γGF model that has been matched to the muoproduction data. Where the charm scale-noninvariance is most important, the calculation is reliable to ~±40%.

We conclude that diffractive charm production is responsible for ~1/3 of the total inclusive scale-noninvariance observed in F_2 in a region bounded by $2<Q^2<13$ (GeV/c)^2 and $50<\nu<200$ GeV and centered at x_B~0.025. A more complete discussion can be found in Ref. 7.

This work was supported by the High Energy Physics Division of the U.S. Department of Energy under Contract Nos. W-7405-Eng-48, DE-AC02-76ER03072, and EY-76-C-02-3000.

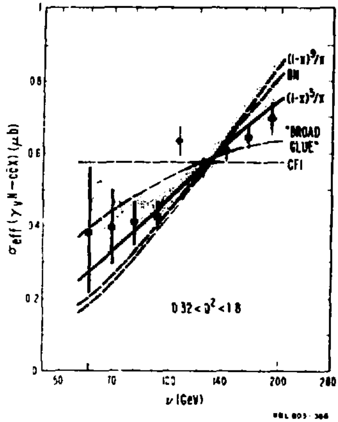

FIG. 3. Energy-dependence of the effective cross section σ_{eff} for diffractive charm production by virtual photons. For $0.32<Q^2<1.8$ (GeV/c)^2, σ_{eff} varies with Q^2 by ≤20%. Errors are statistical. The solid curve exhibits the ν-dependence of the photon-gluon-fusion model with the "counting rule" gluon x distribution $3(1-x)^5/x$, and represents the data with 13% confidence. Other possible models indicated by dashed lines are described in Ref. 7. Curves are normalized to the data. The shaded band exhibits the range of changes in shape allowed by systematic error. For clarity it is drawn relative to the solid curve.

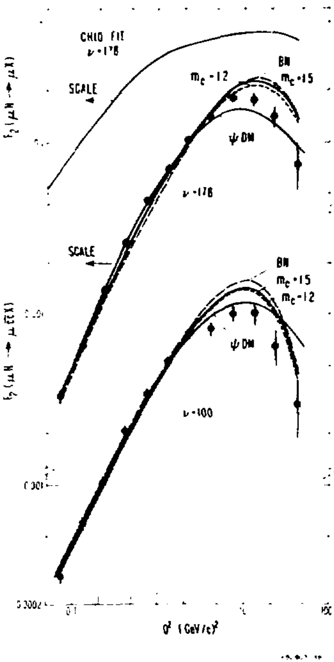

FIG. 4. Q^2-dependence of the structure function $F_2(c\bar{c})$ for diffractive charm muoproduction. At each of the two average photon energies, each curve is normalized to the data. Errors are statistical. The solid (short dashed) curves labelled m_c=1.5 (1.2) exhibit the photon-gluon-fusion prediction with a charmed quark mass of 1.5 (1.2) GeV/c^2. Solid curves labelled ψDM correspond to a ψ-dominance propagator, and long-dashed curves labelled BN are the model of Ref. 8. Shown at the top is a fit adapted from Ref. 9 to the inclusive structure function F_2 for isospin-0 μN scattering. The shape variations allowed by systematic errors are represented by the shaded bands.

FIG. 5. Scale-noninvariance of $F_2(c\bar{c})$. Data points are arranged in pairs, alternately closed and open. The points in each pair are connected by a solid band and labelled by their common average value of $x_B=Q^2/2m_p\nu$. Errors are statistical. The dashed lines are the prediction of the photon-gluon-fusion model with $m_c=1.5$ GeV/c^2 except that the model is renormalized and damped at high Q^2 as described in the text. The solid bands represent the slope variations allowed by systematic errors.

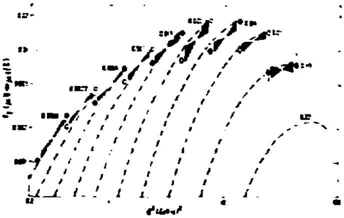

ν(GeV)	27	42	67	106	168	
Q^2 (GeV/c)^2	$\frac{10^4\partial F_2(c\bar{c})/\partial \ln Q^2}{10^4\partial F_2(\mu N)/\partial \ln Q^2}$					x_B
0.63	17 / 1070	30 / 1090	43 / 1110	54 / 1120	58 / 1130	
1.0	23 / 980	43 / 1010	65 / 1040	77 / 1050	84 / 1060	0.002
1.6	30 / 650	59 / 680	87 / 700	107 / 720	115 / 730	0.003
2.5	36 / 310	73 / 340	110 / 350	139 / 363	145 / 360	0.005
4.0	36 / 320	80 / 390	128 / 430	162 / 460	163 / 480	0.008
6.3	29 / 210	75 / 330	128 / 410	165 / 460	154 / 490	0.013
10	15 / 50	54 / 220	104 / 340	138 / 430	112 / 480	0.020
16	4 / -130	27 / 50	64 / 230	90 / 360	52 / 440	0.032
25	-2 / -189	7 / -126	26 / 50	40 / 230	0 / 570	0.050
40	0 / -31	-1 / -171	6 / -122	10 / 50	-22 / 240	0.080
65		0 / -23	1 / -154	1 / -119	-16 / 50	0.130

Table II. Calculated $10^4\partial F_2/\partial \ln Q^2$ at fixed x_B vs ν (top), Q^2 (left margin), and x_B (diagonals, right margin). For each Q^2-ν combination, two values are shown. The bottom value is from a fit to the structure function F_2 for μN scattering (Ref. 9). The top value is the contribution $F_2(c\bar{c})$ to F_2 from diffractive muoproduction of bound and unbound charmed quarks.

REFERENCES

1. A.R. Clark et al., Phys. Rev. Lett. 43, 183 (1979).
2. A.R. Clark et al., Phys. Rev. Lett. 45, 686 (1980).
3. A.R. Clark et al., LBL-11562 (to be submitted for publication).
4. K. Schilling, P. Seyboth and G. Wolf, Nucl. Phys. B15, 397 (1970).
5. See these proceedings, H. Miettinen, "Soft Hadron Physics".
6. A.R. Clark et al., Phys. Rev. Lett. 45, 682 (1980).
7. A.R. Clark, et al., LBL-10879, submitted for publication.
8. F. Bletzacker and H.T. Nieh, SUNY-Stony Brook Report No. ITP-SB-77-44 (unpublished).
9. B.A. Gordon et al., Phys. Rev. D20, 2645 (1979).